8 Convection in lakes

8.1 Introduction to convective mixing in lakes

The first phenomenon, which comes in mind, when addressing convection, is the cooling-induced mixing in the surface layer during cold nights. There are, however, four scenarios where heat fluxes in the boundary layer cause temperature (and/or salinity) changes, which lead to water column instabilities and finally trigger convection. Therese four processes are (Figure 9.1):

- **Cooling-induced** density-instabilities and subsequent turbulence at the **surface** ($T > T_{MD}$)
- **Evaporation** at the water surface of **salty water bodies**
- **Warming-induced** density-instabilities and turbulence at the **surface** (also under-ice, $T < T_{MD}$)
- **Warming-induced** density-instabilities and turbulence in the bottom boundary layer.

However, convectively-driven turbulence occurs in natural waters not only due to heat fluxes but also under several more circumstances, which are discussed below: In general, convective turbulence occurs when any density-modifying process manoeuvres or produces **heavier water on top of lighter water**. As an example: evaporation in salty waters causes higher salinity / higher density at the very top of the water body, which leads to instabilities. Another example: the formation of bubbles at the sediment reduces the density at the bottom of the water column and leads to upward bubble plumes (= mixture of water and gas).

In this chapter, we discuss - after the classic cooling-induced convection - the following convection phenomena, which occur in lakes (Figure 9.1):

- **Shear-induced** benthic convective instabilities in **bottom boundary layers** (Section 9.5)
- Convective turbulence caused within **thermobaric-instabilities** (Section 9.6)
- Local instabilities (layering) caused by **double diffusion** (Section 9.7)
- **Bioconvection** induced by motile plankton (Section 9.8).

References, where convective processes in lakes are presented:

Wüest A., and Lorke, A. (2003) Small-scale hydrodynamics in lakes. *Annual Reviews of Fluid Mechanics*, **35**: 373-412.

Bouffard, D. and A. Wüest (2019). Convection in lakes. *Annual Reviews of Fluid Mechanics*, **51**: 189 – 215. Doi: 10.946/annurev-fluid-010518-040506.

Sommer, T., J.R. Carpenter, and A. Wüest (2014). Double-diffusive interfaces in Lake Kivu reproduced by direct numerical simulations. *Geophysical Research Letters* **41**(14): 5114–5121, doi: 10.1002/2014GL060716

Sommer, T., F. Danza, J. Berg, A. Sengupta, G. Constantinescu, T. Tokyay, H. Bürgmann, Y. Dressler, O.R. Sepulveda Steiner, C.J. Schubert, M. Tonolla, and A. Wüest (2017). Bacteria-induced mixing in natural waters. *Geophysical Research Letters* **44**(18), 9424–9432, doi:10.1002/2017GL074868

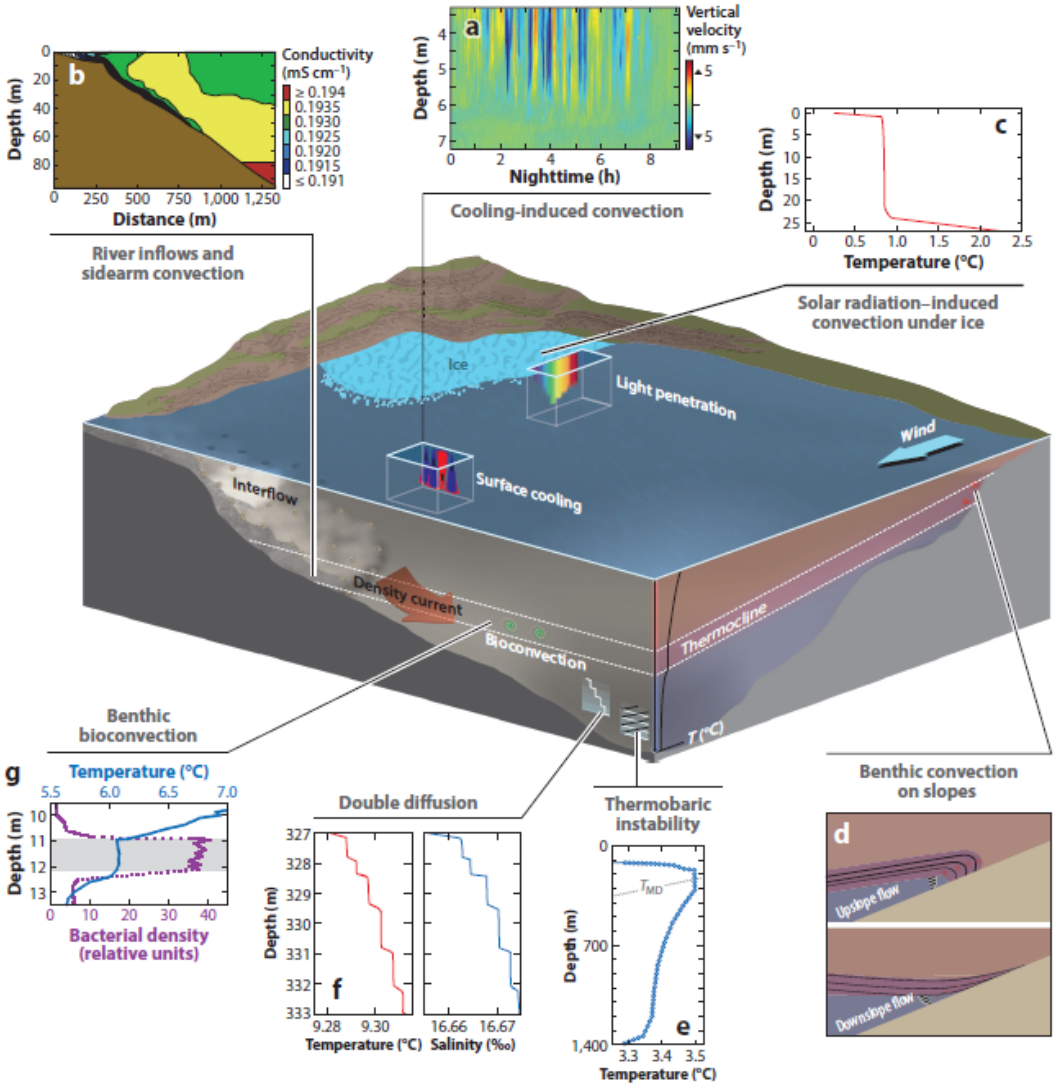

Figure 9.1 – *Schematics of convective processes shown in this chapter: (a) cooling-induced convection at night, (b) river inflows and sidearm convection, (c) solar radiation–induced convection under ice, (d) shear-induced benthic convection, (e) thermobaric instability, (f) double diffusion, and (g) bioconvection. Figure from Bouffard and Wüest (2019).*

8.2 Energetics of convective instabilities

a) Onset of convective instabilities – definition of Rayleigh number

We can analyse thermal convection for flow stability and transition to turbulence. In analogy to the **Reynolds number**, there is a non-dimensional number, which expresses the ratio of destabilising to stabilising forces acting on the water column. This ratio is called ***Rayleigh number.***

Acting forces:

destabilising: negative buoyancy (gravitation) as a result of the negative stratification; force: $g\ \Delta\rho/\rho = g\ \alpha \Delta T$

stabilising: viscosity ν and heat diffusivity D (slow down and smooth).

Comparing the three effects above, by using time scales as the comparative scale (L = thickness of the unstable zone considered):

viscous time scale: $T_\nu = L^2/\nu$

diffusive time scale: $T_D = L^2/D$

inertial time scale: $T_N = 1/N$.

(N = stability frequency = Brunt-Väisälä frequency; see chapter "*Density*"). Instabilities occur, if density exchange by upward and downward buoyancy is faster than the spreading of velocity fluctuations (effects of viscosity) and the spreading of temperature fluctuations (effect of molecular heat diffusion). In quantitative terms, convective turbulence starts if:

$T_N^2 << T_\nu T_D$ or $\frac{T_\nu T_D}{T_N^2} >> 1$

Replacing the time scales with the definitions above, leads to the following non-dimensional number:

(9.2.1) $$\frac{T_\nu T_D}{T_N^2} = \frac{L^4 N^2}{\nu D} = \frac{gL^3 \Delta\rho/\rho}{\nu D} = \frac{g\alpha \Delta T L^3}{\nu D} = Ra$$ = **Rayleigh number >> 1.**

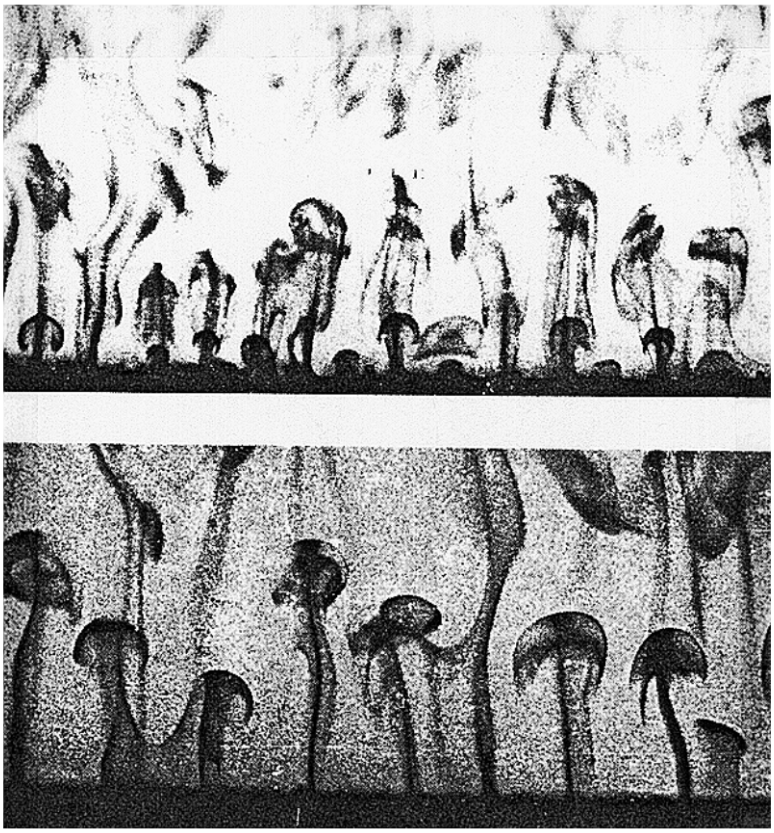

Figure 9.2.1 – *Photographs of "Thermals" rising from a heated horizontal surface. The sinking "Thermals" are*

due to cooling from above. The continuity equation calls for equal masses of water rising and sinking. Figure from Sparrow et al. (1970).

In the last (fourth) term for the definition of Ra (Eq 9.2.1) it has been assumed that the density differences $\Delta\rho/\rho$ are due to temperature inversions $\alpha\Delta T$.

Interpretation

Ra:	ratio of the destabilising effect of buoyancy versus the stabilising effects of molecular viscosity and molecular diffusivity of heat
$Ra < Ra_C$:	laminar (possible only under strongly controlled laboratory conditions)
$Ra \approx Ra_C$:	Rayleigh-Bénard cells or other regular structures form (this can occur also in very slow geological flows)
$Ra \gg Ra_C$:	fully turbulent (omnipresent in reservoirs, lakes, oceans, atmosphere).

Ra_C depends on the geometry of the surface of the fluid body and its spatial extension. In the general case, there are several Ra_C for one set of the experimental arrangement (higher modes, non-stationary flow). The smallest value of Ra_C is theoretically 1708 und confirmed experimentally as 1700 ± 50.

b) Density flux and buoyancy flux for surface convective turbulence

In the surface boundary layer (SBL) convection occurs, when higher density is produced at the very top (right at the surface) of the water column. Higher density is produced by cooling when $T > T_{MD}$, or by warming when $T < T_{MD}$ or by salinity-production via evaporation (chapter "*Density*"). Then, the surface water column becomes unstable and convective turbulence sets in (Rayleigh instability, see above). The net **density (mass) flux** $\langle w'\rho'\rangle = F_\rho$ is directed downwards (heavier parcel moving down and lighter moving up; Figure 9.2.1) and causes a contribution in the **buoyancy flux** term. In the TKE budget (chapter *Hydrodynamics*), the term $J_b = (g/\rho)\langle w'\rho'\rangle$ makes a positive contribution (= production of turbulence → here J_b is a source of turbulence).

The most common way to generate heavier water parcels on top of lighter parcels is by cooling at the water surface (heat loss to atmosphere). The effect of cooling is the formation of small parcels right at the top of the surface, which are slightly cooler than the parcels below. If $T > T_{MD}$ then the slightly cooler parcels are slightly heavier by $\Delta\rho$ and subsequently sink. Relative to the base of a mixed layer (of thickness h_{mix}), these parcels generate a potential energy (per kg of parcel water mass) given by

(9.2.2) potential energy: $$\frac{g h_{mix}}{\rho}\Delta\rho \qquad [J\ kg^{-1}]$$

where $\Delta\rho$ is the density difference of the water parcel relative to the background density ρ. We assume that the „density producing process" lasts for some time Δt. Then we can express the potential energy release per time Δt (rate of potential energy release; units of power):

(9.2.3) rate of potential energy release: $$\frac{g h_{mix}}{\rho}\frac{\Delta\rho}{\Delta t} \qquad [W\ kg^{-1}]$$

Because the "density" and potential energy release occurs right at the very top of the water column, we call this turbulence production term as (index „o" for surface and „b" for buoyancy):

(9.2.4) surface buoyancy flux $$J_b^o = \frac{g h_{mix}}{\rho}\frac{d\rho}{dt} \qquad [W\ kg^{-1}]$$

This equation can intuitively be interpreted: Assume that the sinking parcels have on average a higher density by $\Delta\rho$. They replace lighter water parcels below (ρ) until the entire mixed layer has a density of $\rho + \Delta\rho$.

We assume that the time interval Δt is needed to replace all the parcels of the mixed-layer with water of density $\rho + \Delta\rho$. You can think of a front of higher density water moving downwards with a velocity of $w = - h_{mix} / \Delta t$ [m s^{-1}] with an associated **density flux** of:

(9.2.5) $F_\rho = w\,\Delta\rho$ [kg m^{-2} s^{-1}]

For a mixed layer of thickness h_{mix} and a rate of density increase of $d\rho/dt$, the change of potential energy per area of the entire mixed layer is given by

(9.2.6) $$F_{pot} = \frac{g h_{mix}^2}{2}\frac{d\rho}{dt}$$ [W m^{-2}]

(the factor 1/2 is due to the vertical integration of $h\cdot dh$ over the entire mixed layer h_{mix}). Using the definition of J_b^o (above) leads to the following relation between F_{pot} and J_b^o:

(9.2.7) $$F_{pot} = \frac{g h_{mix}^2}{2}\frac{d\rho}{dt} = \frac{h_{mix}\rho}{2}\frac{g h_{mix}}{\rho}\frac{d\rho}{dt} = \frac{h_{mix}\rho}{2} J_b^o$$ [W m^{-2}]

8.3 Convection induced by boundary fluxes

a) Quantitative formulation of cooling-induced convective turbulence

The TKE balance in the non-stratified and non-sheared SBL (assuming no other turbulence sources than convection; no large-scale shear) has the simple form (production $J_b(z)$ of TKE = dissipation $\varepsilon(z)$ of TKE):

(9.3.1) $$\varepsilon(z) = J_b(z) = -\frac{g}{\rho}\overline{w'\rho'}(z)\,.$$ [W kg^{-1}]

In Figure 9.3.1 the buoyancy flux is schematically shown for a mixed layer loosing heat at the surface while cooling from temperature $T(t_1)$ to $T(t_2)$. For a homogenous rate of cooling $\partial T/\partial t = [T(t_2) - T(t_1)] / \Delta t$ within the mixed-layer of thickness h_{mix}, the vertical heat flux as a function of depth is given by:

(9.3.2) $$H(z) = c_p\rho\,\overline{w'T'}(z) = c_p\rho\frac{\partial T}{\partial t}(-h_{mix} - z)$$ [W m^{-2}]

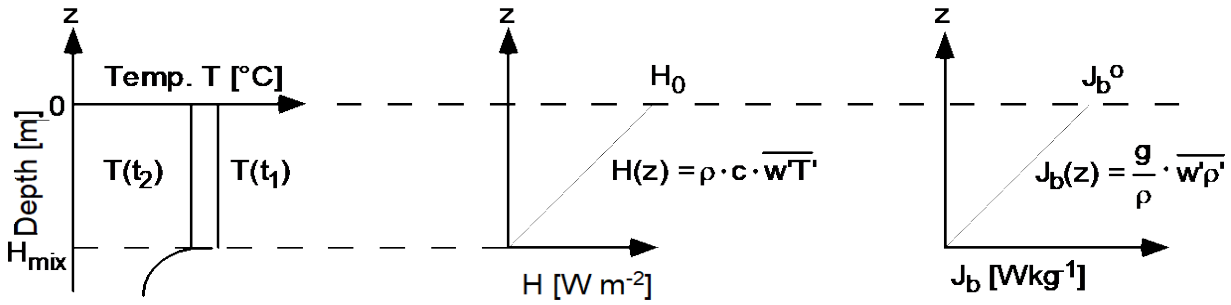

Figure 9.3.1 - *Schematics of the heat flux (middle) and the buoyancy flux (right) as an effect of homogeneous cooling of a mixed SBL of thickness H_{mix} by $\Delta T = T(t_1) - T(t_2)$ during time interval $\Delta t = t_2 - t_1$ (left).*

Temperature T and density ρ are connected via expansivity α: $\partial\rho/\partial T = -\rho\alpha$ (see chapter "*Density*" for definition of α). The same holds for the deviations (fluctuations): $\rho' = -\alpha\,\rho\,T'$. Therefore, the heat flux H(z) and the buoyancy flux $J_b(z)$ are directly related by:

(9.3.3) $$J_b(z) = -\frac{g}{\rho}\overline{w'\rho'} = \frac{g}{\rho}\alpha\rho\ \overline{w'T'} = \frac{\alpha g}{c_p\rho}H(z) \qquad [W\ kg^{-1}]$$

H(z) is positive upwards and ρc_p [J m^{-3} K^{-1}] is the heat capacity. For the example in Figure 9.3.1, where H(z) is linear in z and also $J_b(z)$ is therefore a linear function with depth:

(9.3.4) $$J_b(z) = \frac{\alpha g}{c_p\,\rho}H(z) = \alpha\,g\frac{\partial T}{\partial t}(-h_{mix} - z) \qquad [W\ kg^{-1}]$$

According to eq. 9.3.1, average dissipation $\langle\varepsilon\rangle$ within the mixed layer h_{mix} is therefore $0.5\cdot J_b^o$, as follows directly from inserting the above relations into the definition of the average:

(9.3.5) $$\langle\varepsilon\rangle = \frac{1}{h_{mix}}\int_{h_{mix}}\varepsilon(z)\,dz = \frac{1}{h_{mix}}\int_{h_{mix}}J_b(z)dz = \frac{1}{h_{mix}}\frac{g\,h_{mix}^2}{2\rho}\frac{d\rho}{dt} = \frac{1}{2}J_b^0 \qquad [W\ kg^{-1}]$$

It implies that the average dissipation $\langle\varepsilon\rangle$ is a function of the surface buoyancy flux J_b^o alone. As a consequence, there are only two **relevant physical parameters** defining the similarity scaling for convective turbulence: **Thickness h_{mix} and surface buoyancy flux J_b^o.**

b) Experimental observations

Figure 9.3.2 shows a typical temperature structure (and fluctuations T`) in a fully turbulent and highly convective SBL of the open ocean. The associated dissipation rate $\varepsilon(z)$ decreases as a function of depth quite gradually until the base of the mixed layer is approached, where $\varepsilon(z)$ drops off sharply (~50 m deep in Figure 9.3.2; lower panel). This indicates that the zone immediately below the mixed layer is protected against turbulence from above.

Figure 11.3.2

Convective SBL in the open ocean. ***Left****: vertical temperature profile. Note the temperature fluctuations due to sinking and rising plumes and note the fine resolution of the temperature scale.*

Right*: dissipation profile [W kg^{-1}] in a convective SBL in the open ocean. Note the sharp drop-off at the base of the mixed layer.*

Source: Shay and Gregg (1986).

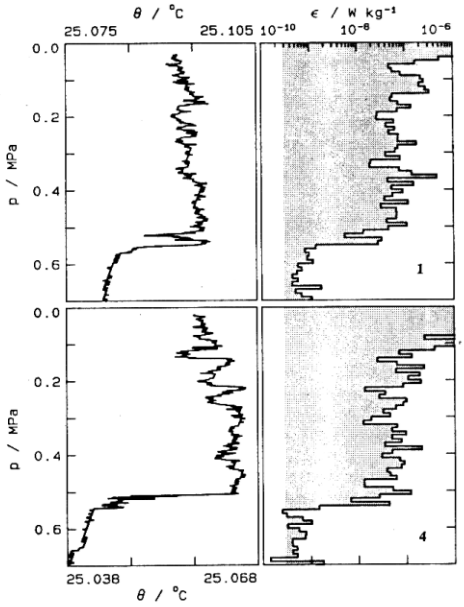

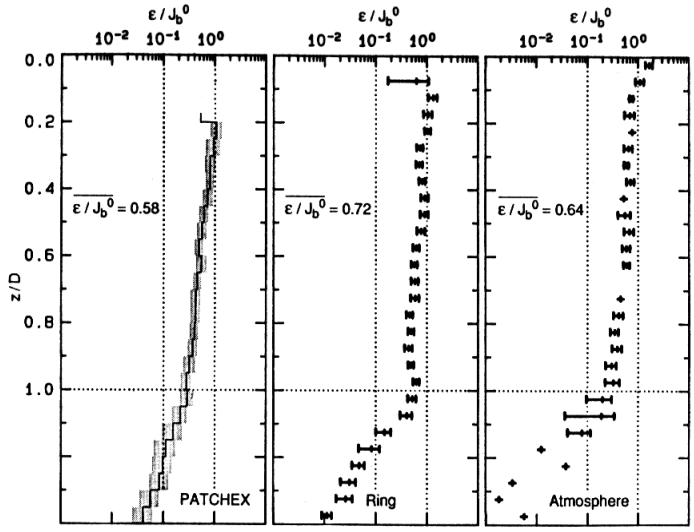

Figure 9.3.3*:* *Similarity scaling* $\varepsilon / \mathrm{J_b^o}$ *for convective turbulence (from Shay and Gregg 1986).*
Left*: quiet region in the open Pacific (Patchex)*
Middle*: in a warm-core Gulfstream ring, during a cold-air outbreak*
Right*: in the atmosphere. Shading and horizontal bars indicate 95% confidence level.*

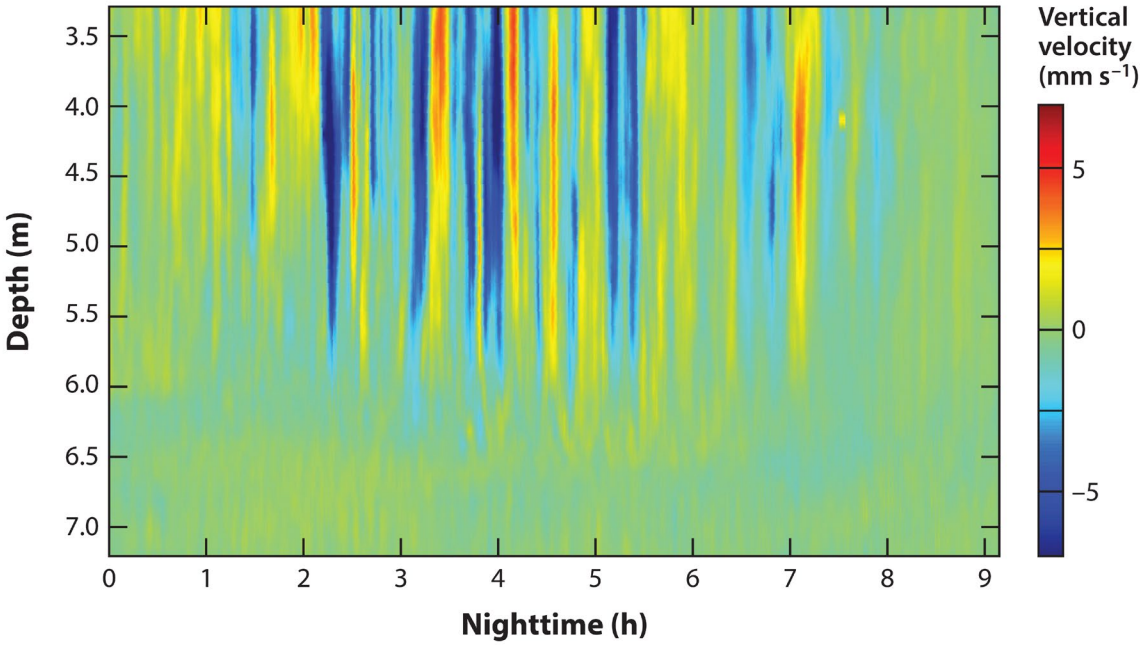

Figure 9.3.4 - *Cooling-induced penetrative convective mixing in the surface layer during night-time hours as observed by vertical velocity measurements in a small lake. The heat map provides visualization of the thermal plumes between 3.3 and 7.2 m depth in the convective mixed layer H_{mix}. Early in the night, we observe rapid deepening of the H_{mix} followed by almost stationary H_{mix}, when the seasonal stratification with large N^2 is reached. Figure from Jonas et al. (2003).*

c) Differential cooling and sidearm convection

The classical thermal convection becomes more complex in small lakes or lakes with dendritic-type shorelines (sidearms). Horizontal density gradients resulting from nearshore shallow water, cooling faster at night than offshore water, trigger a cross-shore transport. This process, called differential cooling is exemplified by the density current that was observed at night by Fer et al. (2002) in Lake Geneva (Figure 9.3.5) The basin-scale relevance of this thermal siphon is the role of differential cooling for wintertime deep mixing. Sidearm convection also transports nutrients, gases, pollutants and the like from the littoral into the pelagic, underlining the role of differential cooling.

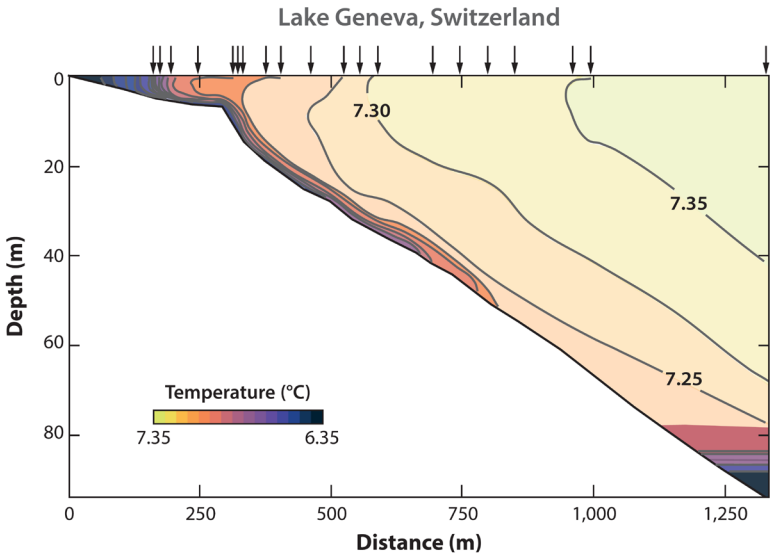

Figure 9.3.5 *- Isotherms derived from CTD profiling (top arrows) indicate a nearshore transect of Lake Geneva, showing a density current induced by sidearm cooling flowing downslope. If scaled up, based on water transport, buoyancy flux, and lake bathymetry, this process would lead to a downward cross-shore transport of ~11 times that of the Rhône River during winter. Figure from Fer et al. (2002).*

d) Sources of buoyancy flux

The buoyancy flux is a source- or sink-term in the turbulent kinetic energy (TKE) balance. The sign of the buoyancy flux has the following meaning (for the TKE balance):

$J_b^o > 0$: Production of TKE (i.e., sinking heavier water parcels or rising lighter water parcels),

$J_b(z) > 0$ in the entire SBL.

$J_b^o < 0$: Strengthening the stratification; no turbulence is produced, hence $J_b(z) < 0$ in the SBL.

The following processes can lead to a positive buoyancy flux and therefore to convective mixing, both at the water surface or within the water column:

(i) **Heat flux at the water surface** (H_{net} = heat flux from the water surface to the atmosphere, α: thermal expansivity, ρc_p = specific heat; index "o" = surface)

$$J_b^o = \frac{g h_{mix}}{\rho}\frac{d\rho_o}{dt} = -g h_{mix}\,\alpha\frac{dT_o}{dt} = \frac{\alpha g}{\rho c_p} H_{net,o}$$

(ii) **Change in salinity**

$$J_b^o = g h_{mix}\,\beta\frac{dS}{dt} = \frac{g\beta}{\rho} m_E = g\beta\, SE = \frac{g\beta}{\rho\lambda_e} H_E$$

($\beta \approx 0.8\cdot10^{-3}$ ‰$^{-1}$ = haline contraction coefficient, S = salinity [‰], λ_e = specific latent heat [J kg^{-1}]; H_E = latent heat flux [W m^{-2}], m_E = mass evaporation rate [kg m^{-2} s^{-1}], E = evapo. rate [m s^{-1}].

Increasing salinity at the surface increases density and generates turbulence ($J_b^o > 0$). Decreasing surface salinity leads to a negative buoyancy flux. E must then be replaced by precipitation, ice melting, or freshwater addition (inflow).

(iii) **Heat fluxes through the water-sediment boundary**
($H_{net,B} > 0$ means heat flux into the water and index B depicts bottom)

$$J_b^B = -\frac{gh_{mix}}{\rho}\frac{d\rho_B}{dt} = gh_{mix}\alpha\frac{dT_B}{dt} = -\frac{\alpha g}{\rho c_p}H_{net,B}$$

(iv) Remineralisation of salts:
negative buoyancy flux ($J_b(z) < 0$), leads to stabilization.

(vi) Particles settling from density currents.
makes water lighter, negative buoyancy flux, leads to stabilization.

e) Convective similarity scaling

We already realized above that convective similarity scaling is determined by two relevant physical quantities. The same conclusion can be drawn from **dimensional analysis** of the quantities involved:

J_b^o	[W kg^{-1} = m^2 s^{-3}]	surface buoyancy flux
ε	[W kg^{-1} = m^2 s^{-3}]	dissipation rate of TKE
h_{mix}	[m]	thickness of well-mixed SBL
w_*	[m s^{-1}]	velocity of the rising / sinking thermals.

This analysis shows that there are only **two independent dimensions**: lengths (m) and time (s). Therefore, from the list above, only two physical quantities are independent from each others (see “Buckingham theorem”). A reasonable (and independent) choice is:

J_b^o and h_{mix},

as these two quantities define in fact the physical setting. The dimensional analysis leads to the following relations (always modulo non-dimensional factors f_1 to f_4 which need to be determined experimentally; dimensional analysis does not provide absolute scales):

Dissipation:	$\varepsilon_* = f_1 \cdot J_b^0$
Velocity of thermals	$w_* = f_2 \cdot (h_{mix} \cdot J_b^0)^{1/3}$
Depth of convection:	$L_* = f_3 \cdot h_{mix}$
Time scale for one full cycle	$T_* = f_3 \cdot h_{mix} / (f_2 \cdot (h_{mix} \cdot J_b^0)^{1/3}) = f_4 \cdot (h_{mix}^2 / J_b^0)^{1/3}$

Further quantities (such as the inverse temperature gradient $\partial T/\partial z$; eddy diffusivity K_{con} in the mixed layer, etc.) can be deduced based on scaling with only J_b^0 and h_{mix}.

f) Monin-Obukhov length

As demonstrated in laboratory experiments by Deardorff et al. (1969), sinking thermals still have part of their kinetic energy when they reach the bottom of the mixed layer. Consequently, the sinking water parcels can overshoot the density surface at the base of the mixed layer and partly penetrate into the pycnocline below the mixed SBL (***penetrative convection***). A fraction of that energy is available for the ***entrainment*** of heavier water from below into the mixed SBL, leading to ***mixed-layer deepening.*** Finally, a minor part of the energy from the sinking plumes may be transferred into the stratified water below via internal waves. Experimental evidence shows that all together up to 30% of the released potential energy by surface cooling (production of TKE) can end up by increasing the potential energy of the stratified water column.

Convective turbulence is not the only agent for the entrainment of thermocline water into the surface mixed layer; another source is provided by wind stirring. The relative importance of these two processes changes with depth h: the effect of the wind is inversely proportional to depth (h), whereas the effect of convection decreases more gradually with depth (almost constant). For the sake of simplicity, it is assumed that the turbulence level for convective mixing is constant with depth and that $f_1 = 1$. The ***Monin-Obukhov Length*** L_M (see Figure 9.3.6 for definition) is defined as the depth $h = L_M$ at which the two quantities $\varepsilon = J_R$ (wind) and $\varepsilon = J_b^0$ (convection) are equal:

$$L_M = -\frac{u_*^3}{kJ_b^o} = -\left(\frac{\rho_{air} C_{10}}{\rho}\right)^{3/2} \frac{W_{10}^3}{kJ_b^o} \quad . \qquad [m]$$

The negative sign is chosen by convention in order to distinguish this situation from the case with negative buoyancy flux J_b^0 (warming of the water column). Note that the major contribution to entrainment is convection if $L_M < h_{mix}$ and wind if $L_M > h_{mix}$. A schematic diagram of all the quantities discussed is provided in Figure 9.3.6. Since L_M decreases with increasing α, and thus with water temperature T, entrainment in temperate lakes is usually controlled by cooling. However, when the surface temperature approaches 4 °C, L_M becomes large and wind remains the only stirring agent.

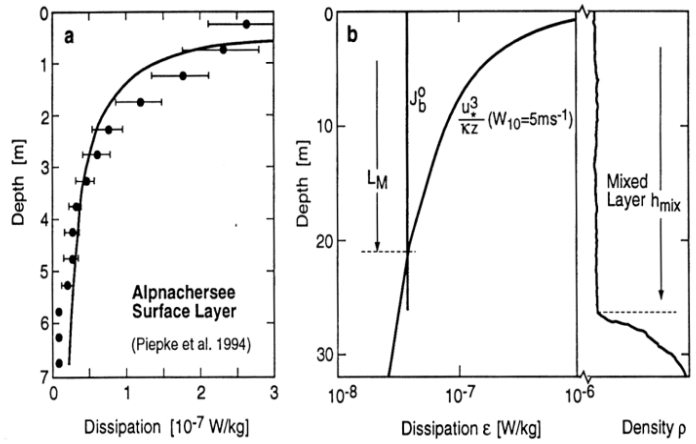

Figure 9.3.6 - ***Left****: Dissipation profile in the SBL of a lake.* ***Right****: Schematic definition of the Monin-Obukhov length L_M in the SBL. If the BBL is convectively mixing, the same concept can be applied for the BBL and a corresponding BBL L_M can be defined.*

8.4 Under-ice radiation

A remarkable type of convection occurs under the ice-cover in late winter (Figure 9.4.1). By then, surface water temperatures are below T_{MD} ($\alpha < 0$) (chapter 2 *Density*) and protected from wind stress. In late winter, as soon as snow disappears from the ice surface, the volumetric radiative warming deposits heat into the top water layer, leading to gravitational instability and convection. As the solar radiation is weak, the resulting buoyancy flux and convectively driven mixing are also weak. The radiatively-driven under-ice convection differs from the classical convection by (a) that the forcing is a

volume source, in contrast to the surface cooling, and (b) the convective mixed layer (CML) is separated from the ice by a thin, stable diffusive layer of thickness δ (inset in Figure 9.4.1). Yet, the CML is characterized by the thermal plume velocities and the subsequent deepening of the CML, both of which are dependent on solar radiation and on the light absorption. In situ observations typically reported $w_* \approx 1–7$ mm s^{-1} and CML-deepening rates of ~0.5 m day^{-1} reaching up to 3 m day^{-1} for strong solar radiation and weak background stratification. Similar to the case $\alpha > 0$, differential heating between the littoral and pelagic zone can lead to large-scale circulation (Ulloa 2019).

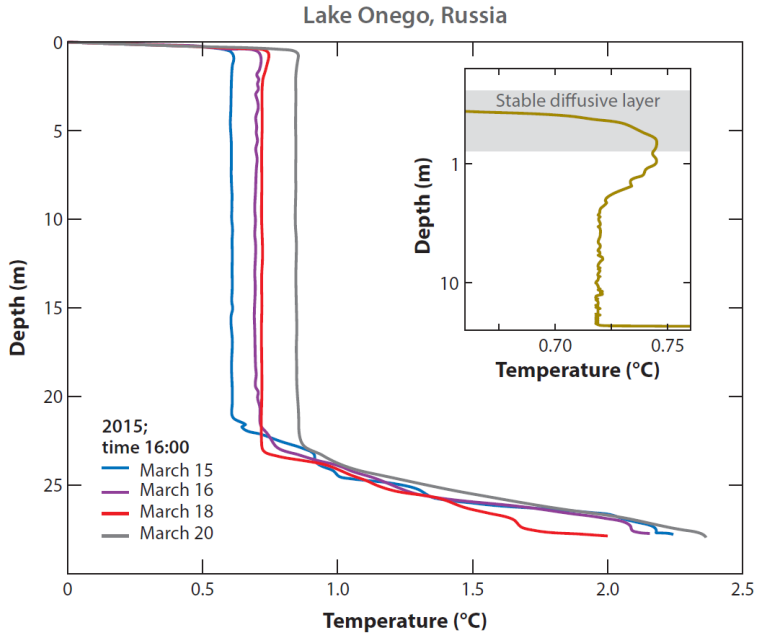

Figure 9.4.1 - Left: Temperature profiles in Lake Onego (Russia) taken at 16:00 (local time) on March 15, 16, 18, and 20, 2015. These profiles show the thermal structure of the radiatively driven convection as well as the layer deepening and increasing the background potential energy. **Inset:** The under-ice diffusive boundary layer (in log scale). Figure from Bouffard et al. (2016).

8.5 Shear-induced benthic convection over slopes

The setting for the shear-induced convection in the bottom boundary layer (BBL) is illustrated in Figure 9.5.1. In stratified basins, winds excite omnipresent basin-scale internal seiches. The subsequent periodic bidirectional flow leads to alternating shear above the lakebed. As indicated in Figure 9.5.1, the effect of the back-and-forth flow of the stratified layers causes a periodic variation in the stratification of the sloped BBL. During the upslope flow phase, the layer directly above the sediment moves slowly (no slip at sediment) compared to water some distance above the sediment (Figure 9.5.1). Hence, the more distant water travels a longer distance parallel to the tilted lakebed compared to near-sediment water (differential advection). Given the background stratification, the denser water parcels

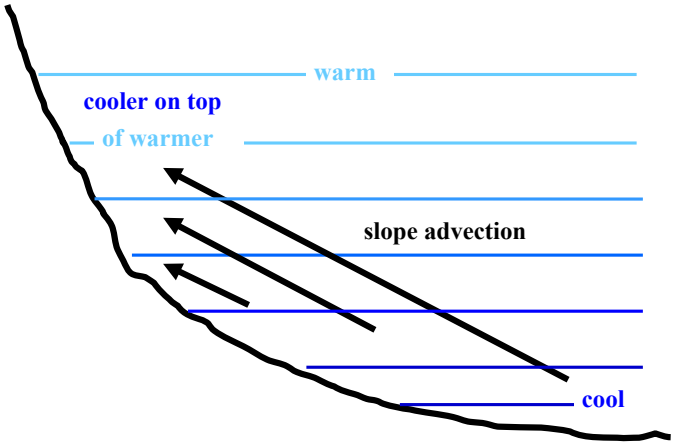

Figure 9.5.1 - *Schematics of the generation mechanisms for shear-induced instabilities within the BBL. Due to the shear gradient in the BBL (see arrows) and the stratification of the water column, cooler water can be sheared on top of warmer water (longer arrow brings denser water from deeper reaches).*

from greater depth end up on top of the shallower and lighter water and cause instabilities, as exemplified in Figure 9.5.2 (Lorke et al. 2005). During the opposite downslope flows, half a seiche period later, shallow, lighter water moves on top of heavier water (which results in enhanced stratification directly above the sediment (Figures 9.5.1/2).

An observation of seiches within parallel-slope temperature gradients is documented in Figure 9.5.2. Analogous to boundary-induced convection, the level of turbulence can be characterized as a function of height h above the sediment by the buoyancy flux $B(h)$, which is defined by the covariance of the vertical velocity w' and density ρ' fluctuations (see above) and can be quantified by ($\partial\rho = -\rho\alpha\,\partial T$)

$$B(h) = -\frac{g}{\rho}\overline{\rho' w'} \approx \frac{g}{\rho} h \frac{\partial \rho}{\partial t} = g\alpha h \frac{\partial T}{\partial t} = g\alpha h u \frac{\partial T}{\partial x}. \qquad \textbf{(9.5.1)}$$

For this approximation, it is assumed that the downward density flux leads to a homogeneous density increase over the convective mixed layer (CML) of thickness h in the BBL. Equation 9.5.1 is consistent with our expectations that shear-induced convective turbulence increases with α, current u, thickness h, and the along-slope temperature gradient $\partial T/\partial x$ (values in Figure 9.5.2) The practical implications are that strongly excited basin-scale seiching (u) causes a thicker CML with stronger convective turbulence. Unsurprisingly, this process has first been observed in the ocean, where ocean currents u (tides) are much stronger than in lakes. Given that all lakebeds are sloped and seiching in enclosed waters is omnipresent, we can expect that most BBL are also mixed by shear-induced convection. Convective mixing in the BBL has biogeochemical implications in and above the sediment, as oxygen is brought close to the sediment and redissolved solutes (nutrients) are removed from the sediment surface. As an overall effect, the exchange of biogeochemical constituents between the stratified interior and the BBL is intensified.

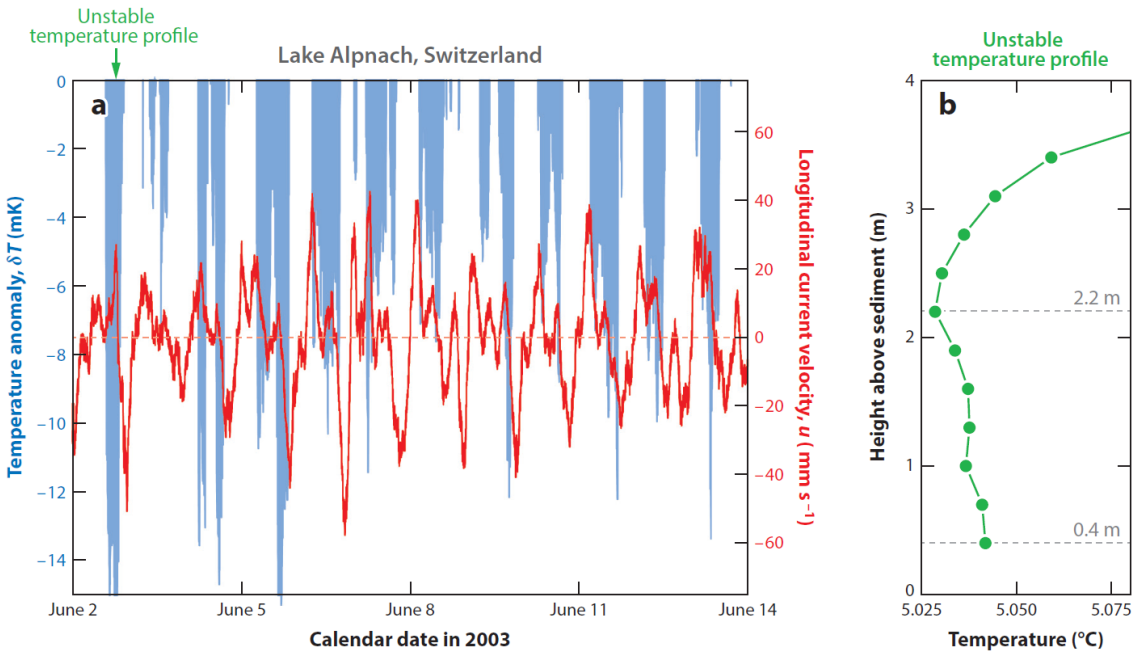

Figure 9.5.2 - *Shear-induced convection above a lakebed with slope of ~0.006 and a parallel-slope temperature gradient ∂T/∂x = 0.1°C/250 m. Together with the convective layer height h = 2.5 m, the maximum current velocity of the seiching u = 3 cm s^{-1} and the thermal expansivity α = 24×10^{-6} °C^{-1} (for 5.5 °C water) result in an upper bound of the buoyancy flux B(h) ≈ 7×10^{-9} Wkg^{-1}.* ***Left (a):*** *A twelve-day time series of the along-lake current velocity u (red line, right scale) and temperature anomaly δT (light-blue shading, left scale) in the bottom boundary layer (BBL) of Lake Alpnach at 31 m depth. The anomaly δT is the temperature difference between 2.2 and 0.4 m above the sediment (two dashed lines in panel b). Positive upslope currents lead to negative δT (blue shading), causing unstable stratification (positive δT with stable BBL not shown).* ***Right (b):*** *An example of an unstable temperature profile (time indicated by the green arrow in panel a). Figure from Lorke et al. (2005).*

8.6 Convection by thermobaric instabilities

Stratification of the Lake Baikal waters has some peculiarities specific to cold, deep lakes. For more than half of the year (including ~3½ months of ice cover), the surface water cools from above and stratifies the uppermost water column (Figure 9.6.1). Because T_{MD} is ~4 °C at atmospheric pressure, the cooler surface water is lighter and floats on the warmer, and therefore heavier, water below (where the thermal expansivity, $\alpha > 0$). The lower bound of the surface layer is determined by the temperature of maximum density T_{MD}, which is a function of depth (Figure 9.6.1).

The deep-water masses are not much affected by the seasonal changes at the surface, and it remains permanently (classically, with temperatures above T_{MD}) stratified throughout the year. The requirement for stable stratification implies that the vertical temperature gradient changes sign exactly at the depth at which the in situ temperature meets T_{MD} (where $\alpha = 0$), as exemplified in Figure 9.6.1. Evidently, at this crossover, the temperature has its local maximum (by definition, as $\partial T / \partial z$ changes sign; Figures 9.6.1/2), the so-called mesothermal maximum. As explained in Figure 9.6.2, this is the only temperature profile that is consistent with stable stratification. Any vertical displacement of the mesothermal maximum away from the

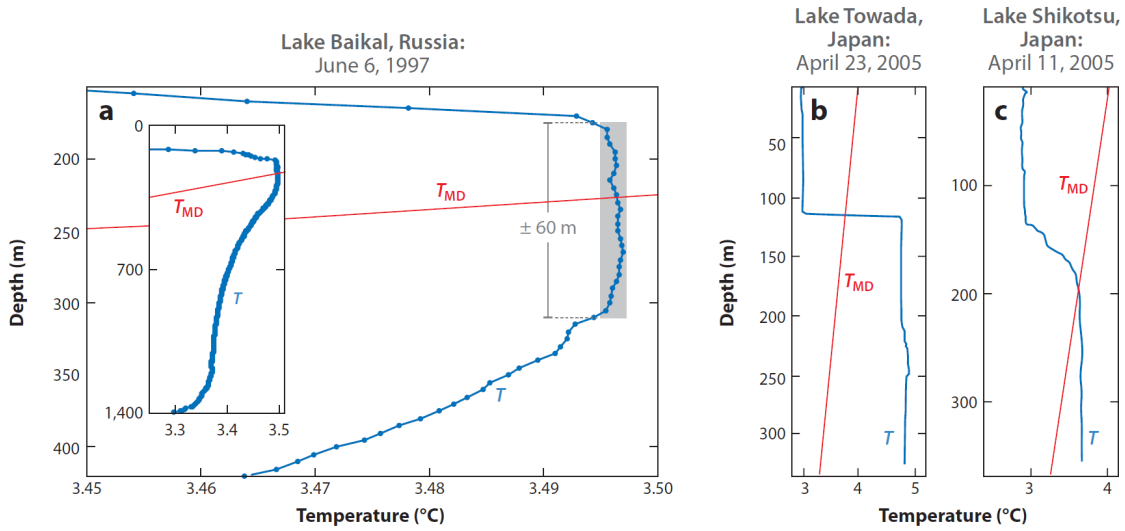

Figure 9.6.1 - *Thermobaric instability at the mesothermal maximum of deep lakes. (a) Temperature (T) profile in Lake Baikal on 6 June 1997, indicating the cold inversely stratified surface layer (above 200 m depth), the permanently stratified deep water (below 300 m depth), and the homogenized layer where the mesothermal temperature maximum crosses the line of T_{MD}. The uniformity at 230 ± 60 m is a result of thermobaric convective mixing.* ***Inset:*** *Depiction of the entire T profile. (b) T profile from 23 April 2005 in Lake Towada, where T crosses T_{MD} = 3.8 °C at ~110 m depth. (c) T profile from 11 April 2005 in Lake Shikotsu with the corresponding crossover at 3.6 °C at ~200 m depth. Figures from Wüest et al. (2005) and from Boehrer et al. (2009).*

T_{MD}-line leads locally to a so-called thermobaric instability, which is a very specific form of convective turbulence, as it depends on the pressure dependence of pure water properties.

Specifically, this instability is caused by the pressure dependency of the thermal expansivity α (p). The mechanism is schematically explained in Figure 9.6.2. Consider the stable temperature profile in the upper panel with the mesothermal maximum on the T_{MD}-line: If there is an upward displacement of the water column (i.e., a baroclinic uplift as indicated by the dotted line in Figure 9.6.2b), the fluid between the mesothermal maximum and T_{MD} has a negative thermal expansivity (i.e., $\alpha < 0$ compared with $\alpha > 0$ before the uplift) and is subsequently unstable throughout the grey-shaded layer in Figure 9.6.2b. The stability is $N^2 < 0$ by definition because the temperature gradient remains $\partial T / \partial z > 0$, whereas α changes to $\alpha < 0$.

A symmetrical situation results from a downward baroclinic displacement of the water (Figure 9.6.2c). In the grey-shaded layer, the temperature gradient remains negative, whereas α changes to positive, and subsequently, the stability is again $N^2 < 0$. From the schematics in Figure 9.6.2, we can generalize that the fluid between the mesothermal maximum and the T_{MD} line is always unstable. From this result, we can draw two conclusions. First, the mesothermal maximum will be exposed to some weak convective turbulence most of the time because the water column is never at rest and some baroclinic motion occurs during all seasons. Therefore, the mesothermal maximum is not a well-defined maximum, but rather a well-mixed layer of almost homogeneous temperature (Figure 9.6.1). Second, the thickness of the well-mixed layer provides an indication for the largest amplitudes of the vertical baroclinic displacement at that depth. Particularly in June, at the end of the inversely stratified winter period, the aftermath of thermobaric instability is well documented in the CTD profiles. From Figure 9.6.1 we can conclude that the vertical displacements at 300 m were limited to ±60 m relative to the equilibrium depth during winter/spring 1997. According to such reasoning, Figure 9.6.1 implies that vertical displacements are limited to only ~60 m.

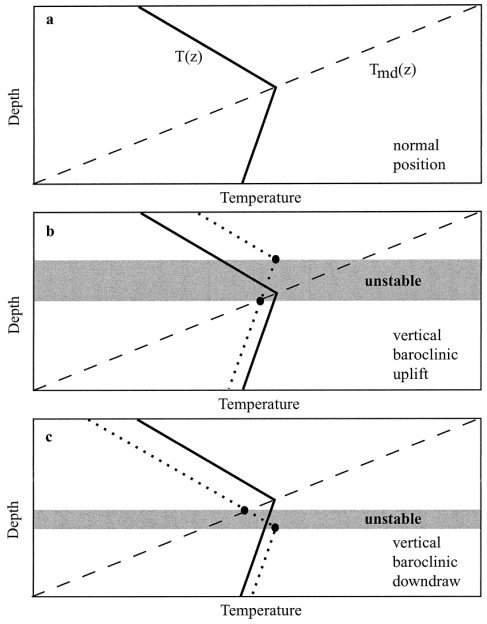

Figure 9.6.1
Schematics of the generation of thermobaric instabilities in the top 350 m of Lake Baikal during winter and spring (Figure 11.6.1).

***Top:** Idealized stable situation, T and T_{MD} cross at meso-thermal maximum*

***Middle:** instability caused by a baroclinic uplift of the water layers relative to T_{MD}*

***Bottom**: instability caused by a baroclinic downdraw of ten water layers. Detailed explanations in text.*

8.7 Convection by double diffusion in stable stratification

Double diffusion (DD) has been found in various geophysical settings and even occurs within stars. In lakes, DD plays a role in two different ways. Active DD convection in stratified waters is usually conjectured when well-defined quasi-homogeneous horizontal layers are observed. These layers are separated by thin and strongly stratified interfaces in overall stable water columns (Figure 9.7.1).

DD convection occurs when three conditions are fulfilled: (a) The vertical density profile must depend on at least two constituents with opposing contributions to stability N^2 (one stabilizing, one destabilizing). (b) These two contributions to the overall stability $N^2 > 0$ are of similar absolute magnitude. (c) The two constituents have substantially different molecular diffusivities (e.g. $D_T \approx 1.4\times10^{-7}$ and $D_S \approx 2\times10^{-9}$ m^2 s^{-1} for temperature and dissolved substances, respectively). We show below that weak background turbulence is usually also a requirement for DD to become dominant. The faster-diffusing constituent (temperature) generates local instabilities in the overall stable density profile, and the produced buoyancy flux drives the DD convection. The physical setting is framed by two stratification parameters: the water column stability N^2 and the density ratio R_ρ, which is the nondimensional ratio of the positive contribution divided by the negative contribution to N^2. Layering is usually found if the range of R_ρ is $1.5 < R\rho < 6$, although DD-favourable conditions exist theoretically over the much wider range of $1 < R\rho < D_T/D_S$.

We occasionally find (bio-)geochemical environments in lakes, where additional constituents stabilize or destabilize the density profiles. Examples of triple diffusion are Lake Nyos (Cameroon) and Lake Banyoles (Spain), where salinity/carbon dioxide and salinity / particles stabilize the water column, respectively. Finally, we discuss below the water column of Lake Kivu, which has two stabilizing components (salinity and carbon dioxide) and two destabilizing components (temperature and methane), representing the most prominent example of quadruple diffusion. We distinguish between fingering convection, where temperature (stabilizing) and salinity both decrease with depth (e.g., Dead Sea), and diffusive-type DD convection, where salinity (stabilizing) and temperature both increase with depth (e.g., Lake Kivu in Figure 9.7.1).

There are various explanations for DD convection. As molecular heat diffusion ($\sim 1.4\times10^{-7}$ m^2 s^{-1}) is ~100 times faster than molecular salt diffusion ($\sim 2\times10^{-9}$ m^2 s^{-1}), the transition zone between the stable interface and the two adjacent well-mixed layers (**Figure 9.7.1**) experiences diffusion-induced changes in temperature but hardly any changes in salinity. This leads to broadening of the *T* interface, and subsequently, this thin transition zone between interface and mixed layer becomes unstable. These instabilities drive in the layers above and below the thermals away from the interfaces (**Figure 9.7.1**), thereby maintaining quasi-homogeneous layers and steep interface gradients. Typical interface steps of temperature and salinity are $\Delta T \approx 10$ mK and $\Delta S \approx 0.013$ with an average interface thicknesses of ~6 and ~9 cm for salinity and temperature, respectively, and average mixed layer heights of ~70 cm (**Figure 9.7.1**). Although these values were observed in Lake Kivu, they are also representative of other lakes and even the Arctic ocean and can be considered typical for lakes. Idealized direct numerical simulations (DNS), together with such observations (Figure 9.7.1b), prove that the vertical fluxes of heat and salt through the core of the interface have a purely molecular nature.

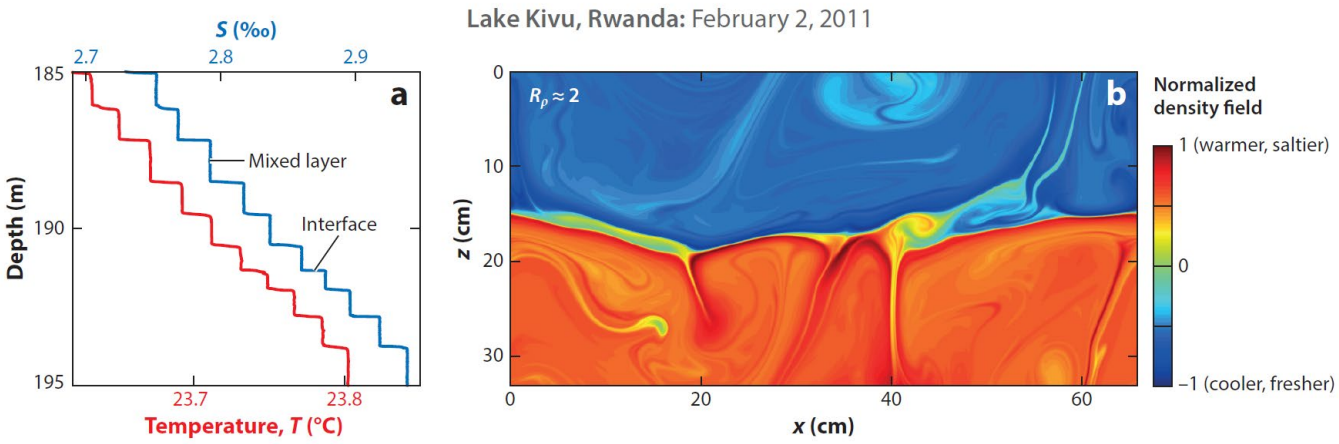

Figure 9.7.1 - *Double-diffusive convection in Lake Kivu. (a) A 10 m long profile section of a double-diffusive temperature (red) staircase and salinity (blue) staircase from February 2, 209. Typical scales of the interfaces are thicknesses of ~6 and ~9 cm for salinity and temperature, respectively, and ~70 cm for the height of the well-mixed layers (for details see Sommer et al. 2013). (b) Convective structures generated by direct numerical simulation for a diffusive-type of double diffusion of a Lake Kivu interface with adjacent mixed layers for Rρ ≈ 2 and realistic background stratification as in panel a. The colours represent the density field (normalized with respect to the mean density and the maximum density difference), with blue for cooler and fresher water versus red for warmer and saltier water. Figure from Sommer et al. (2014).*

8.8 Biologically-induced convection

The question of whether organisms cause mixing in oceans and lakes inspired an enormous laboratory research volume but only limited studies in lakes. To be effective, organisms must overcome geophysically-driven turbulent diffusivities in the stratified ocean interior ($\sim 10^{-5}$ m^2 s^{-1}) or the stratified hypolimnia of lakes ($\sim 10^{-6}$ m^2 s^{-1}). This implies that the product $\langle L'w' \rangle$ of the eddy sizes *L'* and vertical velocities *w'*, generated by aquatic organisms, need to overcome those geophysical diffusivities. From all known observations so far, it appears that biogenic turbulence does not significantly contribute to

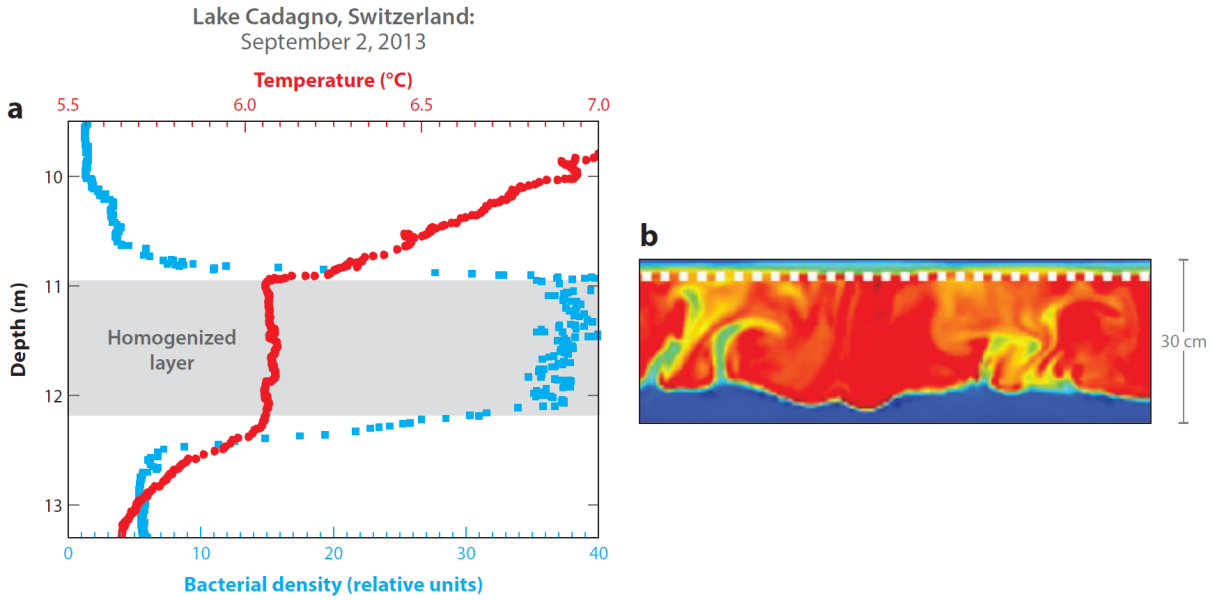

Figure 9.8.1 - (a) Bacteria-induced convection in Lake Cadagno (Switzerland). Temperature (*red*) and bacteria concentration profiles (*blue*) on 2 September 2013, near mid-depth of Lake Cadagno, where autotrophic sulfur bacteria *Chromatium okenii* are densely concentrated at the oxic–anoxic interface. Due to their higher density than water and the ability to swim upward, they cause bioconvection and homogenize a layer (*gray*) more than 1 m thick. **(b)** Direct numerical simulation (DNS) model results showing concentrations of convective plumes in a 30 cm thick layer that developed after 10 hours of DNS, corresponding to the real in situ conditions in August 2015. Details on the figure in Sommer et al. (2017).

mixing or stratification changes. Usually, the generated *L'* are too short to have a macroscopic effect. The mechanical energy is dissipated in the viscous-diffusive envelope around the organisms, implying that swimming-induced fluctuations in velocity and density are evened out before they are advected. While mechanical forcing by organisms may be negligible, there is an alternative to propulsion-induced biogenic turbulence. Bioconvection can be initiated if the microorganisms induce water movements by locally changing the fluid density.

This scenario was found for the upward-swimming purple sulphur bacteria *Chromatium okenii*. These bacteria, with body volumes of V_b and concentrations of C_B, are heavier than ambient water and can mix up to an ~1 m thick layer in a stratified natural lake (Figures 9.8.1). The basic idea is that the bacteria-induced upward net mass flux $w_B(\rho_b - \rho)(V_bC_B)$ (kg m^{-2} s^{-1}) produces potential energy at a rate of $g\rho^{-1}w_B(\rho_b - \rho)(V_bC_B)$ (W kg^{-1}), which is identical to the buoyancy flux rate $B*$ that drives the subsequent convection. The specific conditions found in the lake are $w_B \approx 9\times10^{-6}$ m s^{-1} for the upward-swimming velocity, $(\rho_B - \rho)\rho^{-1} \approx 0.15$ for the density excess of the heavy bacteria, and $V_bC_B \approx 2.5\times10^{-16}$ m^3 × 7.5×10^{10} m^{-3} for the nondimensional ratio of the bacteria volume within the water. For these field-based values, the energy input by the upward-swimming bacteria is $B* \approx 2.5\times10^{-10}$ W kg^{-1}.

DNSs prove that with this level of energy input, the *C. okenii* are capable not only of maintaining the mixed layer but also of gradually expanding this convective layer to several decimetres in thickness (Figure 9.8.1), which is consistent with field observations of up to 1.2 m maximum thickness (Sommer et al. 2017).